



ISTITUTO NAZIONALE DI RICERCA METROLOGICA Repository Istituzionale

A Setup for the Performance Characterization and Traceable Efficiency Measurement of Magnetostrictive Harvesters

This is the author's accepted version of the contribution published as:

Original

A Setup for the Performance Characterization and Traceable Efficiency Measurement of Magnetostrictive Harvesters / Zucca, Mauro; Callegaro, Luca. - In: IEEE TRANSACTIONS ON INSTRUMENTATION AND MEASUREMENT. - ISSN 0018-9456. - 64:6(2015), pp. 0018-9456.1431-0018-9456.1437. [10.1109/TIM.2014.2375711]

Availability:

This version is available at: 11696/31768 since: 2021-02-18T18:52:37Z

Publisher:

IEEE

Published

DOI:10.1109/TIM.2014.2375711

Terms of use:

This article is made available under terms and conditions as specified in the corresponding bibliographic description in the repository

Publisher copyright

IEEE

© 20XX IEEE. Personal use of this material is permitted. Permission from IEEE must be obtained for all other uses, in any current or future media, including reprinting/republishing this material for advertising or promotional purposes, creating new collective works, for resale or redistribution to servers or lists, or reuse of any copyrighted component of this work in other works

(Article begins on next page)

A setup for the performance characterization and traceable efficiency measurement of magnetostrictive harvesters

M. Zucca, L. Callegaro

Abstract— This paper addresses the assessment of the performance and efficiency of direct force magnetostrictive harvesters. A suitable test rig is presented, and its characteristics are discussed. Moreover, this work illustrates some harvester parameters able to influence the measurement results. The setup measures the electromechanical energy conversion properties of direct force harvesters, with a relative expanded uncertainty in the 10^{-3} range for the output power, and 6×10^{-2} for the efficiency. The system has been employed to characterize a novel harvester having a maximum measured efficiency of $\sim 32\%$.

Index Terms— Magnetostrictive devices, Magnetomechanical effects, Measurement techniques, Measurement uncertainty

I. INTRODUCTION

VIBRATIONAL energy harvester devices transform the mechanical wasted energy into electrical energy. Such primary energy can arise from vibration of: machine tools, motors, vehicles, pedestrians walking, etc. The harvesters are usually small sized objects, from MEMS to bulk technology, able of producing power by ten of microwatts to tens of milliwatts. Their use can be envisaged for powering power electronic circuitry or wireless nodes, where the use of wiring cables can be inconvenient or expensive. Today they are popular in transport, in the automotive, in the machine tools, on oil rigs and in the field of structural engineering; more recently also in the bio-engineering field [1].

The comparison among different harvesting devices can be done in terms of efficiency and performance. Mechanical harvesters are usually based on electromechanical apparatus or smart materials such as piezoelectric, magnetostrictive (MST), shape memory alloys, electrostatic, electroactive, etc. [2]. Through the conversion from mechanical to electrical energy it is possible to monitor vibrating contrivances of any kind, by exploiting the mechanical energy engendered by the vibration. To this end, one can use direct force devices inserted in the supports or in the kinematic chain of the vibrating system (machine tools, automotive suspension, etc) or cantilever

devices with seismic masses. This paper focuses on devices of the first type, and the attention is posed on direct force MST harvesters [3-4], where the efficiency and the performance of such devices are considered. The frequencies in play for these applications are in the 10^2 Hz range. For the setup development we focus on a intermediate frequency of 300 Hz.

A MST direct force harvester is a system which exploits the Villari effect. This latter is the change of the material magnetic permeability, which occurs when the material is subjected to a mechanical stress. In some bulk giant MST materials, like Fe-Ga, Fe-Co, Fe-Al, Terfenol-D, etc, this effect is particularly evident. The Villari effect in the energy harvesting is exploited in the following way: when a magnetic bias is induced through DC coils or permanent magnets, a magnetic flux involves the material. This latter reaches a magnetization level which is function of its magnetic permeability. A time varying mechanical stress applied to the material produces on this latter a correspondent variation of its magnetic permeability. As a consequence, the material magnetic flux density has a variation versus time related to the applied stress time behaviour. Due to the Faraday-Lenz law, a pickup coil wrapped around the material and connected to a load is able to harvest an electrical current from the system [5].

In the few papers available in literature (i.e. [3]) some figures of efficiency of such harvesters are presented, but very little is said about the measurement setup used, the parameters of influence and the measurement accuracy. This paper aims to provide detailed information on the implementation of a setup for accurate measurements of the performance and efficiency of a direct force MST harvester, highlighting limitations and merits. The here presented setup is the first of its kind for which it is declared a measurement uncertainty, which is essential for product comparison. It allows to adjust simultaneously, and in an automatic way, the mechanical parameters (load and preload), the operational frequency, the electrical load, while maintaining a sinusoidal mechanical excitation and continuously measuring performance and efficiency. Some improvements will be needed in the future. In particular, some materials (i.e. Fe-Ga) may require a magnetic closure that must

This work was supported by the EU under Decision 912/ 2009/EC. It has been carried out in the framework of the Project EMRP Eng 2, “Metrology for Energy Harvesting”, http://projects.npl.co.uk/energy_harvesting/ EMRP is the EU Metrology Research Programme – 2009.

M. Zucca is with the Electromagnetics Division, INRIM Istituto Nazionale di Ricerca Metrologica, Torino, Strada delle Cacce 91, 10135, Italy (e-mail: m.zucca@inrim.it)

L. Callegaro is with the Electromagnetics Division, INRIM Istituto Nazionale di Ricerca Metrologica, Torino, Strada delle Cacce 91, 10135, Italy (e-mail: l.callegaro@inrim.it).

be provided. In addition, the accuracy of the dynamic mechanical measurements should be improved, which currently limits the accuracy of the setup. However, the results are good and provide a valid support in the development of MST harvesters.

II. QUANTITIES

In this setup the measurands of interest are the efficiency of the harvester and its performance, these latter defined for specific mechanical excitation conditions (frequency, dynamic mechanical stress amplitude, level of the mechanical bias) and electrical load. The characteristics of the coupled electrical circuit (geometrical dimensions, coil turn number, internal electrical resistance of the coil) and the magnetic bias are considered assigned and invariant during test.

In the following the notations below are utilized.

- B_R is the remanence of the permanent magnets.
- σ_0 is the mechanical bias or prestress.
- f is the vibrational frequency.
- R is the load resistance.
- $\delta(t)$ is the displacement time behavior.
- $v(t)$ is the displacement velocity time behavior.
- V is the phasor of the velocity supposed sinusoidal.
- V is the rms value of the velocity.
- K_V is the vibrometer calibration constant.
- $u_V(t)$ is the output voltage time behavior from the laser vibrometer.
- $F(t)$ is the force time behavior.
- F is the phasor of the sinusoidal force.
- F is the rms value of the force.
- K_F is the load cell calibration constant.

- $\Delta\sigma_{pk}$ is the excitation stress amplitude related to F .
- φ_{VF} is the angle between the force and the velocity phasors.
- $p_m(t)$ is the instantaneous mechanical power.
- $i(t)$ is the load electrical current time behavior from the power analyzer.
- I is the rms value of the electrical current in R .
- P_e is the electric active power output.
- P_m is the mechanical active power input.
- $\eta = P_e/P_m$ represents the conversion efficiency.

The performance of the conversion is related to the maximum output power achievable by a device under test. The latter is a quantity related in a complex manner to the electrical and mechanical quantities. A detailed analysis in the case of the performance for magnetostrictive harvesters can be found in [6-7]. Here it is worth to mention how, in order to obtain repeatable measurements, one must check the following quantities: a) type of the active material (magnetic properties and electrical conductivity), b) temperature, c) vibration frequency, d) mechanical bias or preload, e) mechanical coupling between the coil and the active material, f) excitation stress amplitude, g) impedance of the coupled circuit, in addition to the coil resistance, h) state of magnetization of the magnets providing the magnetic bias.

III. EXPERIMENTAL SETUP

A. Setup description

The set-up layout is shown in Fig. 1 and is constituted of five main parts: a) the harvester which includes the magnetostrictive rod, two permanent magnets, the output coil and the load resistance; b) a metallic non-magnetic structure (gantry); c) a

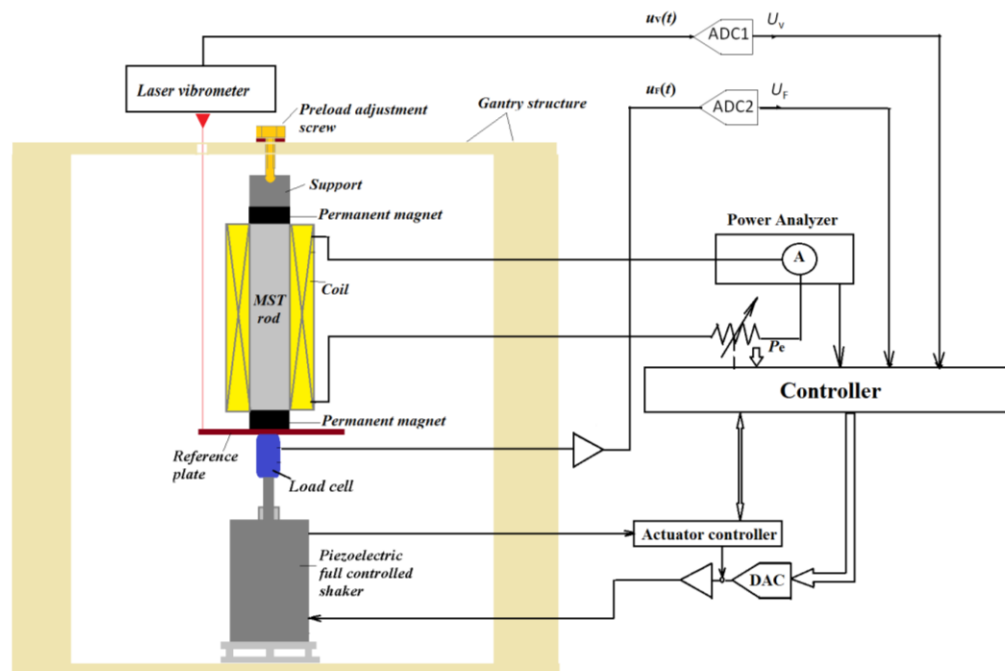


Fig. 1. Scheme of the measurement setup. On the left, the dynamic mechanical chain including, from top to bottom, the mechanical system for the preload adjustment, a support, the harvester, a target plate for the laser doppler vibrometer, a load cell, the excitation actuator. The surrounding electronic circuits for data conditioning and acquisition are also sketched.

- $u_F(t)$ is the output voltage time behavior from the load cell. shaker; d) the measurement transducers and e) the data

acquisition (DAQ) system including a controller.

The gantry is a non-magnetic structure, which has been designed to have mechanical function. It allows to provide a static preload and a dynamic vibrational force to the magnetoelastic material, giving suitable constraints. Undesired resonances in the frequencies range of interest (up to some hundreds of hertz) or mechanical instabilities or drift are avoided by the gantry presence. The frame has natural frequencies far from the ones of interest, being 2.1 kHz the first natural frequency verified for the gantry.

The preload is created by a nut - lock nut system, which press the harvester between the gantry and a piezoelectric full controlled shaker. The latter is fixed on a support, being adjustable in height, which allows a further adjustment of the preload. Screws and supports between different parts are rounded, to facilitate the centering of the parts.

The vibrational dynamic load is created by a piezoelectric shaker. Such actuator includes an embedded displacement strain gage transducer, which drives a controller. So that, a vibrational force having a sinusoidal profile is produced on the mechanical chain. A load cell is placed between the harvester and shaker, being able to measure both the preload and the dynamic load. A small reflective plate is placed closed to the load cell, and allows a velocity measurement in correspondence to the load cell position. Such measurement is made through a laser doppler vibrometer. The harvester coil is closed on a pure resistive load. For a quick characterization of the harvester the load can be constituted by a programmable resistor card, whilst, for an accurate measurement of the performance, Guildline standard resistors are employed. A true rms power analyzer is utilized for the measurement of the output current and the electrical power output is computed through the resistance value.

The system is able to operate producing harmonic vibrations in the frequency range between 100 Hz and 1000 Hz. A mechanical bias up to 2000 N can be settled, this latter superposed to dynamic forces up to 500 N peak at 100 Hz, which are linearly brought down with the frequency increase, up to the maximum of 160 N at 1 kHz. The actuator is actually able to generate greater mechanical forces, however they are limited for obtaining the generation of a harmonic profile, to prevent overheating of the actuator and to comply with the measuring range of the force transducer.

B. •Setup components

- Based windows PC controller.
- NI PXI-PCI8360 to control a PXI board via PCI controller.
- Direct force magnetostrictive harvester (DUT).
- Force measurement: Kistler 9301b load cell (± 2500 N) coupled to a 5018A charge amplifier. <http://www.kistler.com/>
- Velocity: Vibrometer Polytec , OFV 505 sensor head, OFV-5000: VD02 controller.
- Electrical power: WT3000 multimeter from Yokogawa, 2A module.
- Preloaded Full Controlled High Voltage PZT translator. 60

μm open loop travel from 0 to -1000 V, sub-nm resolution, 150 N/ $\mu\text{m} \pm 20\%$ stiffness, 4500/500 N push/pull force, capacity, 660 nF $\pm 20\%$ electrical capacitance, 5.6 KHz $\pm 20\%$ unloaded resonant frequency. 83 ± 0.5 mm total length.

- E-480.00 High Power HVPZT Amplifier, E-509.S1 Sensor/Position Servo Control Module , Sensor - 1 channel version, E-501 Basic Chassis System, E-516.II 1 Channel Computer Interface & Display Module.
- Guildline™ standard resistors (mod. 7320).
- Pickering PXI 40-297-002 programmable precision resistors (1%), max 500 mW (only for the quick determination of characteristics and trends).
- PXI acquisition system: NI PXI-1042Q main frame, NI PXI-8360 (MXI) module (PC link), NI PXI 6143 (ADC1 and ADC2, (16-Bit, 250 kS/s/ch, acquisition and control feedback), NIPXI 6733 (control command to the PI actuator and programmable resistors).
- Labview™ program developed for the purpose.
- Breadboard Thorlabs.

C. Setup operation and data acquisition

The DUT is mounted on the cinematic chain. A nut lock-nut coupling allows the adjustment of the preload σ_0 , which is monitored with the load cell, coupling its amplifier in DC mode. The actuator controller drives the piezoelectric actuator, which applies a force $F(t)$; in all experiments described, $F(t)$ is harmonic. The cinematic stack is bound together by σ_0 (several types of active materials do not allow traction stress to be applied); therefore, the normal operating condition is $|F(t)| < \sigma_0$ and the condition $|F(t)| = \sigma_0$ is an upper DUT drive bound.

During the warm-up time (approx 30 minutes), σ_0 drifts because of the mechanical settlement and relaxation. Thereafter, σ_0 and P_m stabilize. After typically 40 minutes it is possible to start the measurement.

The electrical load of the pickup coil R is set and the load cell amplifier is set to AC mode. The load cell amplifier output voltage $u_F(t)$ is sampled by ADC1 at 50 kHz sampling frequency (higher than the signal bandwidth), and the samples are processed by the controller. The vibrometer output voltage is sampled by ADC2. The sampling is synchronous with the driving frequency. The instantaneous mechanical power is computed as

$$p_m(t) = K_F u_F(t) K_V u_v(t)$$

and the active mechanical power is computed as the average of $p_m(t)$ over 10 signal periods.

The electrical power $P_e = R \cdot I^2$ is computed from the measurement of I given by the power analyzer. P_e and P_m allow to compute the efficiency η of the DUT.

After the measurements, the preload is verified by releasing the stack. This makes difficult to repeat, in separate sessions, two measurements with exactly the same preload value.

IV. DEVICE UNDER TEST

The DUT here considered, described in detail in [7], is constituted by a rod of $\text{Tb}_{0.3}\text{Dy}_{0.7}\text{Fe}_{1.92}$, being 60 mm long and

having a average cross section of 118 mm², provided by Etrema Inc. It is topped at both ends by NdFeB permanent magnets and surrounded by a pick-up coil having 540 turns and internal resistance equal to 4 Ω. The DUT scheme is included in Fig. 1.

The pick up coil is suspended, in order to avoid contacts between the coil and the magnetostrictive material. In fact the friction is a complex nonlinear phenomenon, which reduces the measurement accuracy of the mechanical power and the measurement repeatability. The harvester has been tested with two different configurations, each one with a different material sample and a different permanent magnet couple. In the following the two configurations are named “Harvester #1” and “Harvester #2”. The second is equipped with magnets having a remanence B_R equal to 1.24 T, higher than the remanence $B_R = 1.10$ T of the first sample.

V. RESULTS

Figs. 2 and 4 show an example of DUT characterization under the following conditions: sinusoidal force excitation having stress peak equal to 125 N (peak to peak 250 N), corresponding to $\Delta\sigma_{pk} = 1.05$ MPa; mechanical bias respectively equal to 3.0 MPa, 6.7 MPa and 10.2 MPa; excitation frequency equal to 300 Hz.

The performance, as shown in Fig. 2, significantly varies by varying the mechanical parameters.

There is an important correlation between the mechanical bias and the amplitude of the dynamic force, even for the purpose of optimizing performance. Specifically, the performance increases when the amplitude of dynamic excitation is close to the mechanical bias, taking into account the constraints defined in Sect. III C. Such a phenomenon is widely discussed in [7] together with a complete parametric analysis of the device behaviour. A modelling approach of the problem is presented in [5].

During the measurement, the excitation frequency and the amplitude of the mechanical excitation are kept constant. With the supplied pick up coil, the harvester electrical load equal to 7 Ω optimizes the delivered electrical power; it is the same at the three preload values. The points corresponding to the maximum performance are highlighted on the diagram of Fig. 2 by the letters A, B and C.

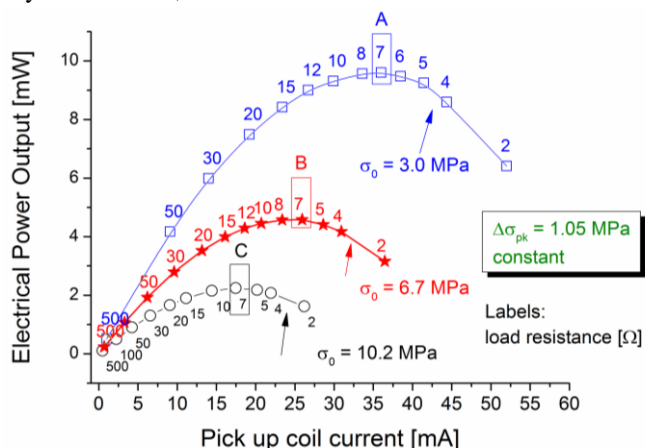


Fig. 2. Performance behavior vs load current measured at 300 Hz for three different preload values, at constant mechanical excitation and frequency. Harvester # 1

Fig. 3 illustrates, for the points A, B and C of Fig. 2, the corresponding time behaviour of the excitation force, of the displacement of the actuator spindle and of the output current. Fig 3 a) shows how the excitation is constantly produced in the three test conditions and the time behaviour of the force profiles is overlapped for cases B and C, while a slight distortion appears in case A. This is due to the fact that as one approaches the critical condition $|F(t)| = \sigma_0$, the system tends to become less stable and also the generation of the excitation force is affected. To guarantee the accuracy limits, discussed in the next section, the system is usually provided with a mechanical bias at least triple with respect to the dynamic excitation peak.

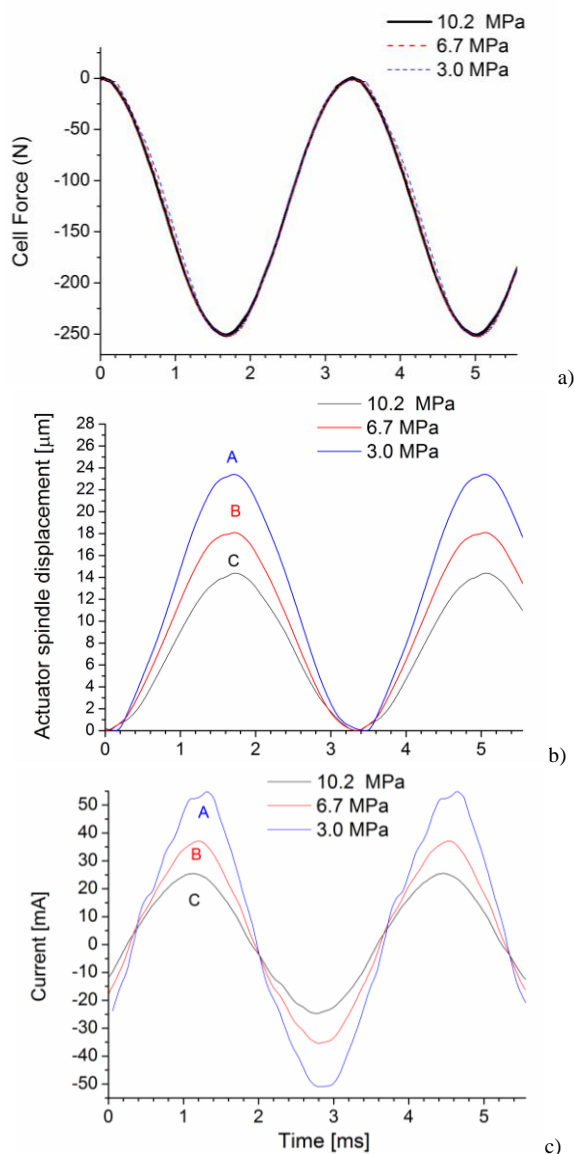


Fig. 3. Time evolution of some quantities involved in the measurement on the DUT described in Sect. IV: a) Force $F(t)$, b) displacement $\delta x(t)$, c) current $i(t)$. Harvester #1.

Fig. 3 b) shows how the greater is the compression given by mechanical bias, the lower is the deformation of the active material being equal the applied excitation force. This is indirectly evident in terms of displacement of the actuator spindle. Also in this case, the more one is far from the critical condition the more the deformation (and consequently velocity and acceleration) is harmonic. Finally, Fig. 3 c) illustrates the waveforms of the output current.

Fig. 4 shows, for the two considered configurations, the estimates and the corresponding intervals of confidence (see Sec. VI) for the efficiency versus the output current. Two main outcomes arise from the results. The first: the efficiency is strongly dependent on the electric load as well as the performance, even if the highest efficiency occurs for a different load with respect to the optimal performance (10 Ω rather than 7 Ω). The second: the configuration Harv. #2, which presents a highest magnetic bias, also has a higher efficiency. This was already known for the performance [7]. Conversely, no significant changes of the DUT efficiency have been measured versus the mechanical preload or the excitation amplitude. By way of example, the Fig. 5 shows in the case of Harv. #2 the variation of the efficiency as a function of the dynamic force amplitude, under optimal load conditions. The difference between the maximum efficiency in Fig. 4 (point “D”) and Fig. 5 is due to the preload variation σ_0 .

Lastly, it is worth to underline how the measured mechanical

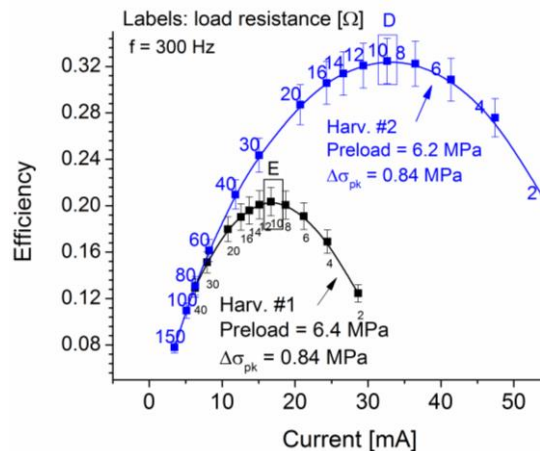


Fig. 4. Efficiency behavior vs load current measured at 300 Hz for the two harvester configurations.

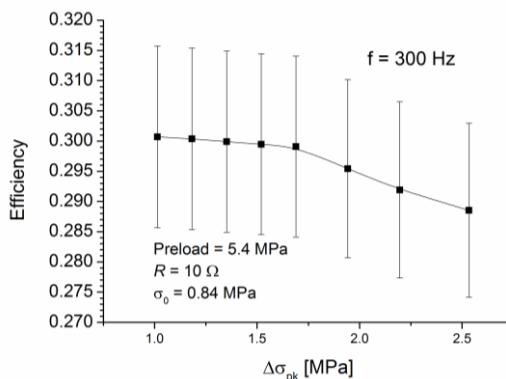


Fig. 5. Efficiency behavior vs the mechanical excitation amplitude. Harvester #2.

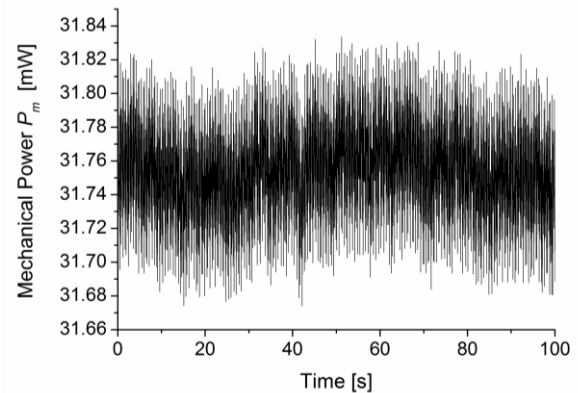


Fig. 6. Values of the mechanical active power versus time. A average point every 30 periods of the instantaneous power is represented (1000 points every 100 seconds). The situation is correspondent of point D in Fig. 5. The electrical power output in the considered time period is constant at 10.2 mW.

power is stable. Fig. 6 shows the minimum oscillation of the mechanical active power measured in a period of 100 seconds, in the conditions of the operating point “D” in Fig. 4. The efficiency is computed from the mechanical and the electrical power estimated for corresponding time frames, therefore the small variations in the mechanical power can be safely neglected.

VI. TRACEABILITY AND UNCERTAINTY

The estimation of the efficiency η values provided in Figs. 4 and 5 was performed with the actual measurement samples. The expression of the corresponding uncertainty $u(\eta)$ with the actual sampled waveforms is very complex (it asks for mathematical tools beyond those employed in the GUM [8] and its supplements). However, considering that the total harmonic distortion of V is lower than 3%, and that of F lower than 2 % for all measured waveforms, we consider that an uncertainty expression performed in the sinusoidal approximation for F and V can be reasonable.

The uncertainty calculation leads to a result of a expanded uncertainty estimated being equal to $6 \cdot 10^{-2}$ with regard to the efficiency. Due to non-linearities and hysteresis of the harvester, the electric power results to be distorted despite the harmonic mechanical excitation. The electric power measurement presents a expanded uncertainty limited to $\sim 10^{-3}$. The accuracy of the measurement setup is therefore related to the dynamic mechanical measurements.

The mechanical power is related to the velocity V and the applied dynamic force F . The measurement model is summarized by Fig. 7 so that the efficiency η is estimated as

$$\eta = \frac{P_e}{V \cdot F \cdot \cos \varphi_{VF}} \quad (1)$$

that is

$$\eta = \frac{P_e}{(K_V \cdot U_V) \cdot (K_F \cdot U_F) \cdot \cos \varphi_{VF}} \quad (2)$$

where

- V is the rms value of the velocity, this latter measured by the vibrometer, having a sensitivity K_V given by its specifications.

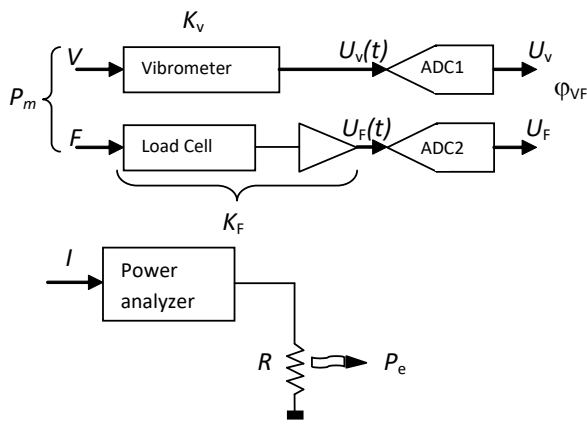


Fig. 7. Uncertainty evaluation model scheme

Its output voltage $u_V(t)$ is sampled by the analog-to-digital converter ADC1.

- F is the rms value of the applied force, measured by the load cell and its front-end amplifier, which can be described with a force measurement constant K_F , calibrated by comparison with an accelerometric system having a known mass m , where the force is computed as the product $m \cdot a$, being a the measured acceleration. The output voltage of the amplifier, $u_F(t)$, is sampled by the analog-to-digital converter ADC2.

The sample set of $u_V(t)$ and $u_F(t)$ allow the calculation of the corresponding rms values V and F and (in a sine wave approximation) the phasor angle φ_{VF} between V and F . Since the mechanical power is mostly reactive, $\varphi_{VF} \approx \pi/2$ and the linear approximation $\cos \varphi_{VF} = (\pi/2 - \varphi_{VF})$ applies. The phase delay introduced by the vibrometer, of about $6 \mu\text{s}$, is numerically corrected, with an uncertainty that translates in an uncertainty of φ_{VF} .

- I is the output current, measured by the power analyzer; the output power P_e is dissipated in a load resistor R .

The uncertainty of all quantities in the measurement model (2) is dependent on both the operating frequency and the magnitude values. For a typical operating condition is given in Table I. It can be seen that the main source of uncertainty is in the measurement of quantities associated to P_m . Since most relevant contributions to the uncertainty come from a Type B evaluation (thus with infinite degrees of freedom) and no single dominant contribution to $u(\eta)$ occurs in Table I, a coverage factor $k = 2$ was considered acceptable in the calculation of the expanded uncertainty.

VII. CONCLUSION

This work proposes a system for measuring the efficiency and the performance of direct force magnetoelastic harvesters. It is the first system of its kind, whose measurement uncertainty was evaluated. The system is able to operate producing harmonic vibrations in the frequency range between 100 Hz and 1000 Hz. Through a screw system and a full controlled piezoelectric actuator, the system can produce a mechanical bias up to 2000 N and the dynamic forces up to 500 N. The setup measures the electromechanical energy conversion efficiency, with a relative expanded uncertainty of the $6 \cdot 10^{-2}$ order. This figure is mainly due to the measurement of the

TABLE I
EXAMPLE OF UNCERTAINTY BUDGET

Quantity	Estimate	Standard uncertainty	Uncertainty contribution
X_i	x_i	$u(x_i)$	$u(\eta)$
R	10.000 Ω	1.5 m Ω	3.1×10^{-5}
I	0.01889 A	11 μA	2.5×10^{-4}
K_V	$5 \times 10^{-3} \text{ m s}^{-1} \text{ V}^{-1}$	$8.65 \times 10^{-5} \text{ m s}^{-1} \text{ V}^{-1}$	3.6×10^{-3}
U_V	0.868 V	0.87 mV	2.1×10^{-4}
K_F	50.00 N V $^{-1}$	0.625 N V $^{-1}$	2.6×10^{-3}
U_F	1.4142 V	1.4 mV	2.1×10^{-4}
$\cos \varphi_{VF}$	0.0556	6.7×10^{-4}	2.5×10^{-4}
η	0.209	Combined standard uncertainty:	5.1×10^{-3}

Operating point: $f = 300 \text{ Hz}$, $F = 70.7 \text{ N}$, $R = 10 \Omega$. Corresponding to the point E in Fig. 5. Harvester #1.

mechanical power, which is particularly critical. The measurement of the performance is rather better with an expanded uncertainty limited to 10^{-3} . The system allows the harvester characterization according to the electric load and the mechanical parameters, highlighting the differences due to the intrinsic device characteristics such as the core dimensions, the material sample and the magnetic bias.

This set-up can contribute to the analysis of the direct force harvester behaviour. It could be utilized, in a near future, for the analysis and comparison of DUT having different magnetoelastic cores, in particular by comparing Terfenol-D, Ni-Mn-Ga and Fe-Ga.

ACKNOWLEDGEMENT

The Authors want to thank P. Squillari for his help in the DAQ user interface development.

REFERENCES

- [1] S. Priya, D. J. Inman "Part V – Selected applications of energy harvesting systems" in Energy harvesting technologies, Springer, 2009, pp. 389-430.
- [2] N. Elvin, A. Erturk, "Chapt. 1 - Introduction and methods of mechanical energy harvesting," in *Advances in energy harvesting methods*, Springer Science & Business Media, 2013, pp. 3-9
- [3] X. Zhao and D. G. Lord, "Application of the Villari effect to electric power harvesting," *J. Appl. Phys.*, vol. 99, pp. 08M703 1–08M703 3, 2006
- [4] Roundy S., "On the effectiveness of vibration-based energy harvesting" *Journal of Intelligent Material Systems and Structures*, vol. 16, no 10, pp: 809-823, 2005
- [5] Zucca, M. and Bottauscio, O., "Hysteretic Modeling of Electrical Micro-Power Generators Based on Villari Effect" *IEEE Trans. Magn.*, vol. 48, no 11, 3092-3095, 2012.
- [6] M. Zucca, O. Bottauscio, C. Beatrice, A. Hadadian, F. Fiorillo and L. Martino, "A study on energy harvesting by amorphous strips", *IEEE Trans. On Magn.*, to be published, DOI: 10.1109/TMAG.2014.2327169
- [7] M. Zucca, A. Hadadian, O. Bottauscio, "Quantities affecting the behavior of vibrational magnetostrictive transducers" presented at the 10th European Conference on Magnetic Sensors and Actuators (EMSA 2014), Vienna, Austria, July 6-9, 2014.
- [8] GUM: JCGM 100:2008, "Evaluation of measurement data — Guide to the expression of uncertainty in measurement," Available online at www.bipm.org, 2008